**IJCTA,** 9(36), 2016, pp. 451-459


# Multiple Instance Learning: Robust Validation on Retinopathy of Prematurity

**Priya Rani* Rajkumar ElagiriRamalingam* Kumar T. Rajamani** Melih Kandemir*** and Digvijay Singh******

***Abstract :*** Retinopathy of Prematurity (ROP) is a potentially blinding disease in the premature infants and requires regular diagnosis and timely treatment. Thus, there is a need for the development of a semi-automated tool which can aid the ophthalmologists in faster diagnosis and treatment. In this work, detection of ROP is performed using multiple instance learning (MIL) approach. In MIL, the image is split into a grid of rectangular patches and features are extracted from each patch. Finally, all the patches belonging to the same image are grouped together and termed as a bag. The bag is given a label depending on whether it is a disease bag or healthy. In this work, four features have been extracted from each image and the bags have been fed into two MIL classifiers: miGraph and citation-*k*NN. The results show that the performance of miGraph is better compared to that of citation-kNN. Thus the results obtained are favorable and demands further work in this field. In our literature review, we observed that there has been no report on use of MIL on detection of ROP. Hence this work forms the basis for the development of a powerful tool for detection of ROP.

***Keywords :*** Retinopathy of Prematurity, Multiple Instance Learning, Scale invariant feature transform, miGraph, Citation-*k*NN.

## 1. INTRODUCTION

Retinopathy of Prematurity (ROP) is a threatening eye disease in premature infants and is one of the leading causes of impairment in children which leads to blindness, if not treated at the right time. The risk factors for ROP include high oxygen supplementation (during initial days) given to the infants for survival, low birth weight (less than 1500 grams) and less gestational period (less than 32 weeks). Usually, the development of the retina takes place after the postmenstrual period in these infants [1]. During this period, ROP interferes with the normal vascular development of the retina; this happens when the blood vessels stop growing till the periphery of the eye, thus developing a demarcation line at the edge of the blood vessels indicating ROP, which is termed as the stage 1 of ROP. This line develops into a ridge (shown in figure 1) marking stage 2, followed by extraretinal fibrovascular proliferation, which is termed as stage 3, wherein new blood vessels proliferate at the ridge, which do not aid in sight. If not treated at this stage, stage 4 begins to develop, wherein the retinal layer starts detaching itself from the choroidal layer, leading to partial retinal detachment, followed by the last stage of ROP, stage 5, where total retinal detachment takes place [2]. In the past two decades, not only the number of premature babies being born has increased tremendously, but their survival rate has also increased. There is also a shortage of the total number of ophthalmologists required on site, to diagnose the disease [3]. Thus a semi-automated tool can help in faster diagnosis of the disease, leading to faster treatment, thus saving the sight of a large number of infants.

* School of Electronics Engineering, VIT University, Vellore-632014, India

** Robert Bosch Engineering and Businesss Solutions, Bangalore, India

*** University of Heidelberg, HCI/IWR, Germany

**** Division of Ophthalmology, Medanta-The Medicity, Gurgaon, India

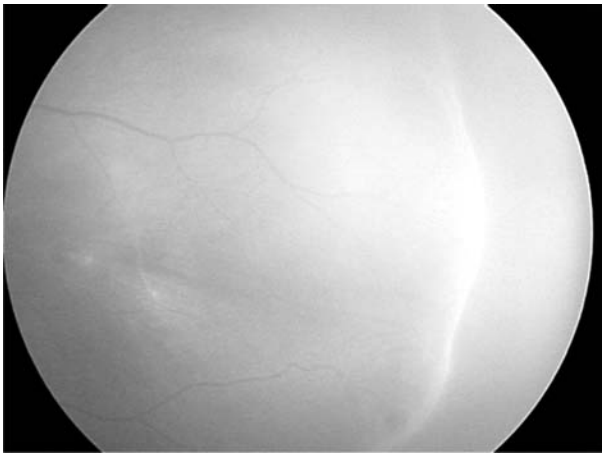

**Figure 1: Figure showing stage 2 of ROP. The ridge develops between the vascular and nonvascular part of the retina, thuspreventing further growth of blood vessels towards periphery**

## 2. LITERATURE REVIEW

Supervised machine learning is the most commonly used approach, where the algorithm takes a set of input data along with its known labels, trains a model based on the data and generates reasonable predictions on a new set of data with unknown labels. But, the disadvantage associated with it is that it needs fine expert labels, which are tedious for medical image analysis applications. The use of weakly supervised machine learning techniques can reduce the expert labeling effort since a common characteristic of the diagnostic images is the locality of particular and characteristic information [4].

Multiple Instance Learning (MIL) was first mentioned by Dietterich et al. [5] when they were investigating a drug prediction problem. In MIL, an image is split into various regular, rectangular patches, and an instance is constructed from each patch by extracting a set of features from every patch. A group of instances which belong to the same image are grouped together into a bag. Labels are assigned to the bags as well as instances. If the classification is at bag level, the labels given to the bags are considered; similarly, if the classification is at instance level, the labels of the instances are of importance. Since, the classification is done at bag level mostly, the label of the bag is assumed as + 1 if it is a positive bag and -1 otherwise. The label of a bag is assumed to be the maximum of the labels of instances in that bag. A negative bag label has all instances within the bag as negative. Whereas, in positive cases, even if the label of atleast one of the instances in a bag is positive, the bag is labeled as positive [4].

There are various reasons why MIL should be chosen for pattern recognition and classification problems. Supervised learning methods demand for ground truth of images (with manual segmentation) during training, which is tedious in case of medical images [6]. Also, a single feature vector is used for supervised learning, which is often restrictive to describe medical images. The use of weakly supervised machine learning techniques not only reduces the effort of creating tedious ground truth for images but also describes the image with more than one feature vector, thus making the task much easier, with decent classification results. Another difficulty with supervised learning approach is to obtain labels on the level of feature vectors (on individual pixels), which is difficult and time consuming, whereas it is comparatively easier to label a full image or some large image regions with a single label. Thus these coarse labeled regions can be used to train a classifier and make predictions at the bag level or instance level [7]. Standard supervised learners receive a "set of instances" which are labeled relevant or irrelevant (positive or negative), whereas multiple instance learners receive a "set of bags of instances" labeled as positive or negative (in case of bag level classification) [7].

There are various multiple instance learning methods developed for various types of applications. One of the important applications is object based image retrieval, where the interest lies in some particular object rather than the whole image. Since MIL can be used to describe the relationship between whole and part of the image, it has been successfully implemented in image retrieval. Changu et al. have presented

a semi-supervised version of MIL, *i.e*. multiple instance semi-supervised learning (MISSL), which takes into consideration both MIL and semi-supervised property at the same time [8]. So, a graph-based multiple-instance learning (GMIL) algorithm has been developed, where in the three kinds of data (labeled, semi-labeled, and unlabeled) simultaneously propagate information on a graph. Another work in the same field has been carried out by Li and Liu, where the first step is based on graph based learning, wherein weights are assigned to each instance on the positive bags alone [9]. In the second step, a ranking score is given to the instances of all the bags in the database. Finally, the images with the largest ranking scores are selected as the retrieval results.

For object detection from images, a boosting algorithm called MILBoost has also been developed [10], which is a combination of MIL with the Viola-Jones method of object detection, which uses Adaboost [11] to create a cascade of detectors, each designed to achieve high detection rates and modest false positive rates. Thus MILBoost produces classifiers with higher detection rates and fast computation times. With a variation in the above algorithm, new algorithms, MIMLBoost and MIMLSVM were formalized for multi-instance multilabel learning, where each training example is associated with not only multiple instances but also multiple class labels [12]. These algorithms can be used in cases where the image belongs to multiple categories, since its semantics can be recognized in different ways.

Kim and Torre have developed a MIL algorithm for Gaussian Processes (GP) called GP-MIL which makes a probabilistic interpretation [13]. It allows bag class likelihood models to be incorporated into the GP framework, which yields non-parametric probabilistic models that can capture the underlying generative process of MIL. Two of the algorithms formulated by Andrews et al. are extensions of Support Vector Machine (SVM) learning, called as mi-SVM and MI-SVM, which make kernel-based classification methods available for multiple instance learning [14]. The first algorithm treats the pattern labels as unobserved integer variables, subjected to constraints defined by the positive bag labels. It maximizes the soft-margin, the jointly over-hidden label variables and a kernelized discriminant function. MI-SVM generalizes the notion of a margin to bags and aims at maximizing the bag margin.

Kandemir et al. have used MIL to study diagnosis of Barett's cancer from hematoxylin and eosin stained histopathological biopsy images wherein the diagnosis is done using graph-based multiple instance learning, known as mi-Graph [15] and the results are appreciable [16]. A weakly supervised classification algorithm for medical images has been presented by Quellec et al. for diabetic retinopathy images [6]. A local relevance score is defined for each sub-image, which is described by a feature vector. In the training phase, the importance of each feature vector in the reference dataset is weighted to adapt the local relevance scores to define it relevant. The local relevance score is high if the patch includes relevant patterns, otherwise it is low. A global relevance score is defined for the image, consisting of the local relevance scores computed for all the sub images of that particular image.

## 3. METHODOLOGY

ROP is a unique disease in itself because the initial stage of the disease (demarcation line) is quite different from the final stage (total detachment of the retina). As shown in figure 1, the retina in premature babies is undeveloped and looks very different from the retina of adults. Moreover, the disease shows different signs compared to the diseases of adults. Thus the algorithms and results obtained for adult diseases (for instance, diabetic retinopathy) cannot be used for concluding in this case. Thus separate study is required to validate and conclude as to which methods and algorithms work best for this particular disease. Previous study in the same area was done on less number of images and the method implemented was miGraph [17]. The results obtained in the previous work were satisfactory, but it had its limitations. Thus in this paper, two MIL methods have been tested and validated on more number of ROP images and classification of the images has been done into ROP and normal. This section includes a short explanation and schematic on the methodology, followed by a sub section on feature extraction, and the last sub-section explains the classifiers, miGraph and citation-kNN, used for the classification of the bags.

As mentioned before, the input image is divided into a grid of rectangular patches. The patch size is calculated by normalizing the size of the image in both *x* and *y* directions by a certain scale value. As the scale value is varied, the classification results also vary. Thus after dividing in the image into rectangular patches, the relevant features are extracted from each of the patch and termed as an instance. Finally, a bag with its instances is given a label and fed into the classifier for classification. The schematic of the proposed methodology is shown in figure 2.

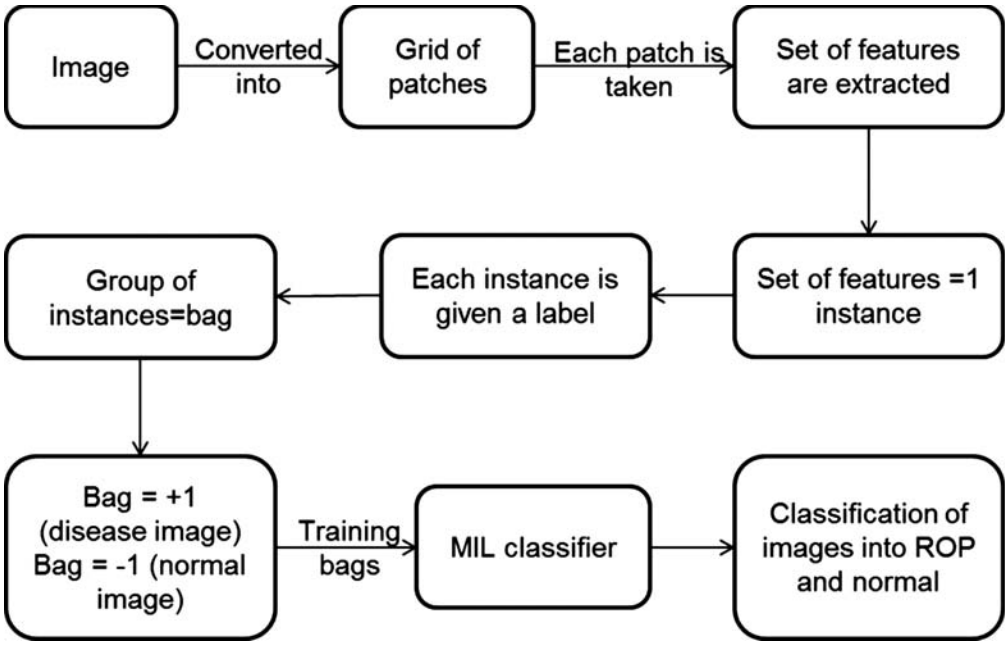


**Figure 2: Schematic diagram of the proposed methodology**

### 3.1. Feature Extraction

To perform classification of the retinal images as ROP affected and healthy, both types of images have been considered. Each image has been split into a grid of rectangular patches by varying the scale value. The features identified and found relevant for this work are color features and texture features. Thus each image patch is represented with: a set of intensity histogram of RGB channels for 26 bins, mean of local binary pattern (LBP) histograms, mean of Scale Invariant Feature Transform (SIFT) descriptors and box count. The description of each of the texture features is given below.

Local binary pattern was first introduced by He and Wang which was a new model of texture analysis based on the texture unit, where a texture image can be characterized by its texture spectrum [18]. Texture unit has been defined as the smallest complete unit, which best characterizes the local texture aspect of a given pixel and its neighborhood in all eight directions of a square raster digital image whereas the occurrence of distribution of texture units computed over a region is called the texture spectrum [19].

Scale invariant feature transform has been proposed by Lowe which has been used to extract distinct invariant features from images to perform reliable matching between different views of the image [20]. It transforms image data into scale-invariant coordinates relative to local features. This approach generates large numbers of features that densely cover the image over the full range of scales and locations. Firstly, keypoints are detected using a cascade filtering approach which uses efficient algorithms to identify candidate locations which are examined in further detail. Once a keypoint candidate has been identified by comparing a pixel to its neighbors, a detailed fit to the nearby data is performed for location, scale, and ratio of principal curvatures. Each keypoint is assigned a consistent orientation based on local image properties. Thus the keypoint descriptor can be represented relative to this orientation and achieve invariance to image rotation. After assigning image location, scale and orientation to each keypoint, a descriptor is computed for the local image region that is invariant to variations such as change

in illumination or 3D viewpoint. Thus large number of keypoints is extracted from images leading to robustness in extracting small objects among clutter. The LBP and SIFT features were calculated using VLFeat library [21].

Box counting or box dimension is one of the widely used dimensions mainly due to its relative ease of mathematical calculation and empirical estimation [22]. To describe it, let F be any non-empty bounded subset of $R_n$ and $N_\delta(F)$ be the smallest number of sets of diameter of maximum size δ that can cover F. Hence to find the box dimension of a plane set F, a mesh of squares or boxes of side δ can be drawn and the number $N_\delta(F)$ can be counted which overlap the set for various small δ. The dimension is calculated as the logarithmic rate at which $N_\delta(F)$ increases as δ tends to 0. It may be estimated by the gradient of the graph of $\log N_\delta(F)$ against $-\log \delta$ [23]. For this work, box count for grid sizes 2,3,...8 has been considered.

### 3.2. Classification

MIL not only provides a learning framework that allows for weak supervision but also handles the locality of the required information. Moreover, the information is localized in diagnostic images [4]. In the case of ROP images, the demarcation line, ridge, extraretinal fibrovascular proliferation and detached retina are localized in the region separating the vascular from the avascular retina. Various MIL methods have been reported and some of them have also been discussed in section 2 of the paper. In this work, detection of ROP has been performed using two MIL methods: miGraph and citation-*k*NN and the results obtained are promising. The formal definition of MIL is as follows: Let the instance space be denoted as X. The data set can be represented as $(X_1, Y_1)$,...., $(X_i Y_i)$, .., $(X_N Y_N)$ where $X_i = x_{i1}$, .... $x_{ij}$, .., $x_{in}$. It consists of the feature set and is referred to as a bag, and $Y_i = \{-1, +1\}$ is the label of $X_i$, where −1 denotes a negative bag and +1 denotes a positive bag [4][15]. Thus with this set of given data, the aim is to use a learner to classify the unseen bags.

#### *3.2.1. Citation-kNN*

Citation-*k*NN is a lazy learning approach, and a modification to kNN algorithm, to adapt it to multiple-instance problems by using modified Hausdorff distance measure [24]. The Hausdorff distance provides a metric function between subsets of a metric space. By definition, two sets A and B are within Hausdorff distance *d* of each other iff every point of A is within distance *d* of at least one point of B, and every point of B is within distance *d* of at least one point of A and the maximum distance or the largest ranked distance is taken as the final measure. The modification thus made to this measure is by considering the *k*-th ranked distance rather than the largest ranked distance. Unlike *k*NN, this method takes into account, not only the neighbors of a bag *b*(according to the Hausdorff distance), called as references, but also the bags that count *b* as a neighbor, called as citers. Thus either references or citers of an unseen example can be used to predict the class of the example rather than only using the references.

**Table 1**

**Distribution of positive and negative bags in R-nearest references and C-nearest citers of an unseen bag [24]**

| *References/Citers* | *Positive bags* | *Negative bags* |
|---|---|---|
| R-nearest references | $R_p$ | $R_n$ |
| C-nearest citers | $C_p$ | $C_n$ |
| Total | $p = R_p + C_p$ | $n = R_n + C_n$ |

The distribution of positive and negative bags in R-nearest references and C-nearest citers of an unseen bag is shown in Table 1, where *p* is the positive bag and *n* is the negative bag. The classification of the unseen bag is defined as: if $p > n$, then the class of the bag *b* is predicted as positive, otherwise it is negative. In case of a tie, the class of bag *b* is predicted as negative. For this work, the number of references was set to 2 and citers were set to 4.

### *3.2.2. miGRAPH*

Zhou et al. proposed miGraph which is different from other methods because it treats the different instances in an image as intercorrelated samples and have shown to exhibit a better performance by exploiting the relations among the instances [15], whereas other methods treat instances in the same bag as independently and identically distributed (I.I.D.) samples, which neglects the relationship among the instances that convey important structure information. In miGraph, each bag is regarded as a graph and each instance is regarded as a node in the graph. This method computes the distance between every pair of node (*i.e*. instances) for a bag. If the distance between two nodes is smaller than a pre-set threshold (set to average distance in the bag), an edge is established between these two nodes, where the weight of the edge defines the affinity between the two nodes. Thus an affinity matrix is derived. Consequently, a graph kernel $k_{bag}$ is designed to capture the similarity among the graphs and is defined as follows:

$$k_{\text{bag}}(\mathrm{X}_b, \mathrm{X}_c) = \frac{\sum_{n=1}^{\mathrm{N}_b} \sum_{m=1}^{\mathrm{N}_c} v_{bn} v_{cm} k_{inst}(x_{bn} . x_{cm})}{\sum_{n=1}^{\mathrm{N}_b} v_{bn} \sum_{m=1}^{\mathrm{N}_c} v_{cm}} \quad (1)$$

where,

$$v_{bn} = \frac{1}{\sum_{u=1}^{\mathrm{N}_b} w_{nu}^{b}} \quad (2)$$

$$v_{cm} = \frac{1}{\sum_{u=1}^{\mathrm{N}_c} w_{mu}^{c}} \quad (2)$$

$\mathrm{X}_b$ and $\mathrm{X}_c$ are two multi-instance bags, $k_{inst}(x_{bn}, x_{cm})$ is an instance level kernel, $v_{bn}$ and $v_{cm}$ are the sum of the weights of the edges incident to nodes (or instances) *n* and *m* of bags *b* and *c* respectively. After designing the graph kernel, the classification problem can be solved by kernel machines. In this work, the kernel machine used for classification purpose is SVM [25]. Thus miGraph method implicitly constructs graphs by deriving affinity matrices and defines an efficient graph kernel considering the clique information. It is a simple, efficient and effective method with low computational cost.

## 4. RESULTS

For the implementation of the proposed method, 56 images were taken-28 with ROP affected and 28 healthy images. The images were obtained from RetCam 120 (Clarity Medical Systems, Inc., Pleasanton, CA) with a field of view (FOV) of 130 degrees from premature infants with gestational period of less than 32 weeks. The proposed experimentation was performed using MATLAB 2013b on Dell Workstation with an *i*7 processor running at 3.40GHz, l6.0 GB RAM. The implementation was done by splitting the data into training set and testing set. There were various results obtained so as to find the best classifier, best split of images into patches, and with the best splits of data. Thus the results have been shown for the classifiers: miGraph and citation-*k*NN. Since the performance of miGraph is better than citation-*k*NN, the results for variation of scales have been shown for miGraph alone. All the results have been shown for the split of data into 50% for training and 50% for testing (Table 2) and also the split into 70% for training and 30% for testing (Table 3) and have been calculated by performing an average of 20 runs. The following six performance metrics have been calculated for MIL classifiers:

- **Accuracy:** Shows the percentage of correctly classified test points.
- **Sensitivity :** Shows the true positive rate (measures the percentage of ROP images correctly identified as ROP).
- **Specificity :** Shows the true negative rate (measures the percentage of healthy images correctly identified as healthy).
- **AUC-ROC :** Shows the area under Receiver Operating Characteristics (ROC) curve.
- **AUC-PR :** Shows the area under precision-recall curve.
- **F1 Score :** Shows the harmonic mean of precision and recall.

**Table 2**

**Table showing the classification results of *miGraph* and *citation-kNN* with scale 4 (split of 50% as training set and 50% as testing set)**

| *Performance matrices* | *Citation-kNN* | *miGraph* |
|---|---|---|
| Accuracy (in %) | 89.64 | 95 |
| Sensitivity (in %) | 96.04 | 97.86 |
| Specificity (in %) | 83.21 | 92.14 |
| AUC-ROC | 0.95 | 0.98 |
| AUC-PR | 0.95 | 0.98 |
| F1 Score | 0.90 | 0.95 |

**Table 3**

**Table showing the classification results of *miGraph* and *citation-kNN* with scale 4 (split of 70% as training set and 30% as testing set)**

| *Performance matrices* | *Citation-kNN* | *miGraph* |
|---|---|---|
| Accuracy (in %) | 93.06 | 97.5 |
| Sensitivity (in %) | 97.22 | 99.44 |
| Specificity (in %) | 88.89 | 95 |
| AUC-ROC | 0.93 | 0.98 |
| AUC-PR | 0.95 | 0.98 |
| F1 Score | 0.93 | 0.97 |

**Table 4**

**Table showing the classification results of *miGraph* with variation in scale (split of 50% as training set and 50% as testing set)**

| *Performance matrices* | *Scale = 3* | *Scale = 4* | *Scale = 5* | *Scale = 6* |
|---|---|---|---|---|
| Accuracy (in %) | 95.36 | 95 | 95 | 95.89 |
| Sensitivity (in %) | 97.5 | 97.86 | 97.14 | 99.14 |
| Specificity (in %) | 93.12 | 92.14 | 92.86 | 92.14 |
| AUC-ROC | 0.98 | 0.98 | 0.98 | 0.98 |
| AUC-PR | 0.98 | 0.98 | 0.98 | 0.98 |
| F1 Score | 0.96 | 0.95 | 0.95 | 0.96 |

## 5. DISCUSSION

In this work, two multiple instance learning methods have been evaluated for detection of ROP in premature infants. The main advantage of using MIL is that it divides the image into a grid of rectangular patches and features are calculated on each patch, thus highlighting the relevant patches, where the important information lies. There are four types of features identified for the images−one color feature and three texture features. The classifiers used for performing classification are mi-Graph and citation-*k*NN. The features extracted were used to classify the images into ROP-affected and healthy, thus detecting the disease in the images. Among other results, the results obtained in this paper using miGraph are better

compared to the last paper [17], proving that more are the images in the dataset, better will be the results obtained. The experiment has been performed by splitting the data into two parts: first, 50% is taken for training and the rest 50% for testing and second, 70% is taken for training and the rest 30% for testing. The results section shows that the latter one gives better results, hence proving that the performance of both the classifiers is better when more data is available for training. Although the results obtained using both methods are appreciable, it should be noted that miGraph gives better performance than citation-*k*NN. Also, dividing of the images into 14patches, by normalizing with the higher scale value leads to increase in the performance of the classifier, thus giving better results as seen in table 4 and 5. In spite of the advantages of splitting the image into rectangular patches, the use of rectangular patches also brings in the non-relevant information of the image as well, into many of the relevant patches, which restricts MIL classifiers from giving their best results. Furthermore, as already mentioned, if the number of input images is increased, there will be an increase in the performance of the classifiers. The main outcome of the work is that MIL works well on the images affected with ROP; hence it can be used to detect the disease in a given number of retinal images obtained from premature infants.

**Table 5**

**Table showing the classification results of *miGraph* with variation in scale (split of 70% as training set and 30% as testing set)**

| *Performance matrices* | *Scale = 3* | *Scale = 4* | *Scale = 5* | *Scale = 6* |
|---|---|---|---|---|
| Accuracy (in %) | 96.11 | 97.5 | 96.39 | 97.22 |
| Sensitivity (in %) | 98.89 | 99 | 99.44 | 99.44 |
| Specificity (in %) | 93.33 | 95 | 92.78 | 94.44 |
| AUC-ROC | 0.98 | 0.98 | 0.99 | 0.97 |
| AUC-PR | 0.96 | 0.98 | 0.99 | 0.96 |
| F1 Score | 0.96 | 0.98 | 0.96 | 0.97 |

## 6. CONCLUSION AND PERSPECTIVES

The literature shows that there is quite less amount of work done for CAD applications with respect to ROP. Moreover, no work has been reported for detection of ROP using MIL methods. Thus this work forms the basis for the development of a powerful tool to be used in CAD applications for automatic detection of ROP and its stages. The good performance of the selected features and the two MIL classifiers motivates further research in this direction. The rectangular patches can be overcome by dividing the image into non-rectangular patches, in such a way that the parts of the homogeneous regions cluster together, thus eliminating the non-relevant parts of the image. More number of features can be added to increase the accuracy of the algorithm. Also, more MIL methods can be tested on the given set of features. The outcome of the work can also be to classify and detect various stages of ROP, thus making it a fully automated system for detection of ROP.

## 7. REFERENCES

1. Hartnett C, O'Keefe M. Screening for Retinopathy of Prematurity. INTECH Open Access Publisher; 2011.
2. IC for the Classification of Retinopathy of Prematurity, et al. The international classification of retinopathy of prematurity revisited. Archives of ophthalmology 2005;123(7):991.
3. Hungi B, Vinekar A, Datti N, Kariyappa P, Braganza S, Chinnaiah S, et al. Retinopathy of prematurity in a rural neonatal intensive care unit in south india: a prospective study. The Indian Journal of Pediatrics 2012;79(7):911–5.
4. Kandemir M, Hamprecht FA. Computer-aided diagnosis from weak supervision: A benchmarking study. Computerized Medical Imaging and Graphics 2015;42:44–50.
5. Dietterich TG, Lathrop RH, Lozano-Perez T. Solving the multiple instance problem with axis-parallel rectangles. Artificial intelligence 1997;89(1):31– 71.

6. Quellec G, Lamard M, Abr`amoff MD, Decenciere E, Lay B, Erginay A, et al. A multiple-instance learning framework for diabetic retinopathy screening. Medical image analysis 2012;16(6):1228–40.
7. Cheplygina V, Tax DM, Loog M. On classification with bags, groups and sets. Pattern Recognition Letters 2015;59:11–7.
8. Wang C, Zhang L, Zhang HJ. Graph-based multiple-instance learning for object-based image retrieval. In: Proceedings of the 1st ACM international conference on Multimedia information retrieval. ACM; 2008, p. 156–63.
9. Li F, Liu R. Graph-based multiple-instance learning with instance weighting for image retrieval. In: Image Processing (ICIP), 2011 18th IEEE International Conference on. IEEE; 2011, p. 2453–6.
10. Zhang C, Platt JC, Viola PA. Multiple instance boosting for object detection. In: Advances in neural information processing systems. 2005, p.1417–24.
11. Schapire RE, Singer Y. Improved boosting algorithms using confidencerated predictions. Machine learning 1999;37(3):297–336.
12. Zhou ZH, Zhang ML, Huang SJ, Li YF. Multi-instance multi-label learning. arXiv preprint arXiv:08083231 2008;.
13. Kim M, Torre F. Gaussian processes multiple instance learning. In: Proceedings of the 27th International Conference on Machine Learning (ICML-10). 2010, p. 535–42.
14. Andrews S, Tsochantaridis I, Hofmann T. Support vector machines for multiple-instance learning. In: Advances in neural information processing systems. 2002, p. 561-8.
15. Zhou ZH, Sun YY, Li YF. Multi-instance learning by treating instances as non-iid samples. In: Proceedings of the 26th annual international conference on machine learning. ACM; 2009, p. 1249–56.
16. Kandemir M, Feuchtinger A, Walch A, Hamprecht FA. Digital pathology: Multiple instance learning can detect barrett's cancer. In: Biomedical Imaging (ISBI), 2014 IEEE 11th International Symposium on. IEEE; 2014, p. 1348–51.
17. Rani P, Rajkumar ER, Rajamani KT, Kandemir M, Singh D. Detection of retinopathy of prematurity using multiple instance learning. In: Advances in Computing, Communications and Informatics (ICACCI), 2015 International Conference on. IEEE; 2015, p. 2233–7.
18. He DC, Wang L. Texture unit, texture spectrum, and texture analysis. Geoscience and Remote Sensing, IEEE Transactions on 1990;28(4):509–12.
19. Ojala T, Pietikainen M, Harwood D. A comparative study of texture measures with classification based on featured distributions. Pattern recognition 1996;29(1):51–9.
20. Lowe DG. Distinctive image features from scale-invariant keypoints. International journal of computer vision 2004;60(2):91–110.
21. Vedaldi A, Fulkerson B. Vlfeat: An open and portable library of computer vision algorithms. In: Proceedings of the international conference on Multimedia. ACM; 2010, p. 1469–72.
22. Feng J, Lin WC, Chen CT. Fractional box-counting approach to fractal dimension estimation. In: Pattern Recognition, IEEE Proceedings of the 13th International Conference on; vol. 2; 1996, p. 854–8.
23. Falconer K. Fractal geometry: mathematical foundations and applications. John Wiley & Sons; 2004.
24. Wang J, Zucker JD. Solving multiple-instance problem: A lazy learning approach 2000.
25. Cluster based Key Management Authentication in Wireless Bio Sensor Network ", ,International Journal of pharma and bio sciences.